

Combining BRITE and ground-based photometry for the β Cephei star ν Eridani: impact on photometric pulsation mode identification and detection of several g modes^{*}

G. Handler,¹ M. Rybicka,¹ A. Popowicz,² A. Pigulski,³ R. Kuschnig,^{4,5}
 E. Zocłńska,¹ A. F. J. Moffat,⁶ W. W. Weiss,⁴ C. C. Grant,⁷ H. Pablo,⁶
 G. N. Whittaker,⁸ S. M. Ruciński,⁸ T. Ramiaramanantsoa,⁶ K. Zwintz,⁹ G. A. Wade¹⁰

¹ Nicolaus Copernicus Astronomical Center, Bartycka 18, 00-716 Warsaw, Poland

² Silesian University of Technology, Institute of Automatic Control, Gliwice, Akademicka 16, Poland

³ Instytut Astronomiczny, Uniwersytet Wrocławski, ul. Kopernika 11, 51-622 Wrocław, Poland

⁴ Institute for Astrophysics, Universität Wien, Türkenschanzstrasse 17, A-1180 Wien, Austria

⁵ Institut für Kommunikationsnetze und Satellitenkommunikation, Inffeldgasse 12/I, 8010 Graz, Austria

⁶ Département de physique, Université de Montréal, C. P. 6128, Succ. Centre-Ville, Montréal, QC H3C 3J7, Canada

⁷ Space Flight Laboratory, University of Toronto, 4925 Dufferin Street, Toronto, M3H 5T6, Canada

⁸ Department of Astronomy and Astrophysics, University of Toronto, 50 St. George Street, Toronto, ON M5S 3H4, Canada

⁹ Institut für Astro- und Teilchenphysik, Universität Innsbruck, Technikerstrasse 25/8, 6020, Innsbruck, Austria

¹⁰ Department of Physics, Royal Military College of Canada, PO Box 17000, Stn Forces, Kingston, ON K7K 7B4, Canada

Accepted 2016 July 17. Received 2016 August 13; in original form 2016 September 10

ABSTRACT

We report a simultaneous ground and space-based photometric study of the β Cephei star ν Eridani. Half a year of observations have been obtained by four of the five satellites constituting BRITE-Constellation, supplemented with ground-based photoelectric photometry. We show that carefully combining the two data sets virtually eliminates the aliasing problem that often hampers time-series analyses. We detect 40 periodic signals intrinsic to the star in the light curves. Despite a lower detection limit we do not recover all the pressure and mixed modes previously reported in the literature, but we newly detect six additional gravity modes. This behaviour is a consequence of temporal changes in the pulsation amplitudes that we also detected for some of the p modes. We point out that the dependence of theoretically predicted pulsation amplitude on wavelength is steeper in visual passbands than those observationally measured, to the extent that the three dominant pulsation modes of ν Eridani would be incorrectly identified using data in optical filters only. We discuss possible reasons for this discrepancy.

Key words: stars: variables: other – stars: early-type – stars: oscillations – stars: individual: ν Eridani – techniques: photometric

1 INTRODUCTION

ν Eridani (HD 29248, $V = 3.92$, B2 III, hence-

forth ν Eri) is arguably the asteroseismically best studied β Cephei star (for more information on this group of massive pulsating variable stars see Stankov & Handler 2005). After an immense ground-based observational effort involving both multisite photometry and high-resolution spectroscopy (Handler et al. 2004, Aerts et al. 2004, De Ridder et al. 2004, Jerzykiewicz et al. 2005, hereinafter JHS), tight constraints on the overall chemical composition and convective core overshooting of this star were obtained, in combination with a detection of differential internal rotation (Pamyat-

^{*} Based on data collected by the BRITE Constellation satellite mission, designed, built, launched, operated and supported by the Austrian Research Promotion Agency (FFG), the University of Vienna, the Technical University of Graz, the Canadian Space Agency (CSA), the University of Toronto Institute for Aerospace Studies (UTIAS), the Foundation for Polish Science & Technology (FNiTP MNiSW), and National Science Centre (NCN).

nykh, Handler & Dziembowski 2004). The latter study as well as alternative models to explain the star’s pulsation spectrum (Ausseloos et al. 2004) additionally pointed towards a necessity for an increase of the iron-peak element opacities.

This success was possible because the star’s pulsation spectrum happened to be very suitable for asteroseismic studies. The pulsations contain a dominant radial mode that immediately constrains the stellar mean density. Furthermore, a triplet of dipole modes was identified observationally, two more $l = 1$ multiplets were found, and a single quadrupole mode was detected. Fitting this observed pulsation spectrum with theoretical models (Pamyatnykh et al. 2004, Ausseloos et al. 2004) revealed that the two lowest-frequency $l = 1$ multiplets correspond to mixed modes, with different contributions from the gravity and pressure mode cavities, which makes the seismic information from them largely independent and complementary.

In addition, low-frequency oscillations likely due to stellar gravity modes were detected (Handler et al. 2004, Aerts et al. 2004, JHS). However, finding excitation of the latter in corresponding stellar models proved to be impossible and would require additional modification to the opacities used for the stellar models (Dziembowski & Pamyatnykh 2008). Finally, Daszyńska-Daszkiewicz & Walczak (2010) applied their method of complex asteroseismology to ν Eri and showed that neither with OPAL nor with OP opacities alone the observed complex amplitude of the bolometric flux variation can be reproduced for both its p and g modes at the same time.

After these studies, the asteroseismic information on the star appeared to be made full use of, at least as far as studies hinged on ground-based data are concerned: the above-mentioned campaigns yielded some 1130 h of time-resolved photometry and 430 h of time-series spectroscopy. Therefore, a return to ν Eri only appeared sensible once new data sets, extensive enough to resolve the pulsation spectrum, and of a quality allowing to decrease the noise level significantly would become accessible.

Such data sets are available nowadays. BRITE-Constellation (Weiss et al. 2014) is a set of five nearly identical nanosatellites with high-quality pointing stability, each hosting a telescope with 30 mm aperture and an uncooled 11 Megapixel CCD, which allows one to acquire time-series photometry of $V \lesssim 4.5$ targets in a 24 degree field of view. Two broadband filters are available, a blue filter with a central wavelength of about 420 nm and a red filter centred at 620 nm. Although these filters do not have the standard Johnson-Cousins bandpasses, their effective wavelengths are similar to those of Johnson B and Cousins R_c , and we therefore name them simply B and R in the remainder of this work.

The satellites are in low-Earth orbits, meaning that they can observe the target fields for up to six months a year and for about 20 minutes per 101-minute orbit, depending on their position with respect to the Sun and the Earth. ν Eri was observed during the second BRITE-Constellation campaign directed towards the field of Orion. In anticipation of these measurements, ground-based photometric observations were organized to coincide temporally. In the following, we report the results of both ground and space-based monitoring.

Table 1. Log of the ground-based photometry of ν Eri.

Observatory	T_{start} HJD – 2456000	T_{end}	# data
Fairborn	943.800	1078.710	1429
SAAO	996.319	1019.347	131

2 OBSERVATIONS AND REDUCTIONS

2.1 Ground-based photometry

Photoelectric time-series measurements in support of BRITE were organized for two reasons. First, their analysis can be directly compared with that of JHS, and second, near-ultraviolet photometry that BRITE cannot provide, is invaluable for the identification of the pulsation modes of β Cep stars. Our ground-based data were obtained at two observatories. The bulk of the measurements originated from the 0.75-m Automatic Photoelectric Telescope (APT) T6 at Fairborn Observatory in Arizona. In addition, the 0.5-m telescope at the South African Astronomical Observatory was employed (observer EZ). Differential time-series photoelectric data were collected through the Strömgen *uvy* filters, and the “classical” comparison stars μ Eri (HD 30211, B5IV, $V = 4.00$) and ξ Eri (HD 27861, A2V, $V = 5.17$) were used. Table 1 gives a summary of those observations; the time base is 135 d.

The data were reduced in a standard way, starting by correcting for coincidence losses, sky background and extinction. Standard extinction coefficients for the observing sites were used. As μ Eri is a known variable star (e.g., see Jerzykiewicz et al. 2013), and has also been observed simultaneously by BRITE-Constellation, these data were set aside for a separate analysis and only the differential magnitudes (ν Eri – ξ Eri) were analysed further. As a final step, the timings for this differential light curve were corrected to the heliocentric frame.

Given that there was no constant star in the observing sequence, we cannot directly specify the accuracy of these observations. However, experience with measurements taken under similar conditions (e.g., Handler et al. 2012) suggests that the rms accuracy per single data point should be well below 4 (u filter) and 3 mmag (v and y filter), respectively.

2.2 BRITE-Constellation

The data were obtained with four out of the five satellites: BRITE-Austria (hereinafter BAb), BRITE-Lem (BLb), BRITE-Heweliusz (BHr), and BRITE-Toronto (BTr). The first two satellites observe through the blue filter, the latter two use the red one (hence the suffixes “b” and “r” in their respective abbreviations). The data for each target are downloaded from the satellites in subrasters of (usually) 28×28 pixel size. Initial photometric reductions are carried out with a pipeline that takes into account bad pixels, median column counts, image motion and PSF variations (see Pablo et al. 2016, Popowicz 2016 and Popowicz et al. 2016).

The data reported here were delivered to the user in the form of ASCII files that contain the HJD of the observations, stellar flux counts, x and y position of the stellar profile on the raster, CCD temperature and a quality flag.

The information aside from HJD and counts is required for data decorrelation. In brief, pixel-to-pixel and intrapixel sensitivity variations modify the measured stellar flux depending on the x/y position on the chip. Temperature variations within the satellites and hence also of the detector during the orbit and on longer time scales also introduce apparent modulations in the signal derived from the initial CCD photometry. These effects may also be intermingled, as the temperature changes also modify the optical system, and the stellar PSFs are large and of varying shape. Therefore, temperature-induced changes of the PSF also modify the relation between the x/y position and the distribution of the PSF over the individual pixels (discussed in detail by Buysschaert et al. 2016). Therefore, BRITE photometry needs to be carefully decorrelated for these factors before proceeding to scientific analyses of the intrinsic stellar variability. The basic process of decorrelation of BRITE data has been described in detail by Pigulski et al. (2016).

In case of constant stars or short-period low-amplitude variables, decorrelation can be performed directly on the data. However, for ν Eri intrinsic stellar variability dominates the light curves. Therefore, decorrelation was carried out in two steps. First, bad points were discarded (according to the data quality flags) and a preliminary frequency analysis was carried out on the light curves from the individual satellites. A multifrequency fit consisting of the detected signals was determined and subtracted from the data. Consequently, the residuals were inspected for correlations, and the latter removed on a step-by-step basis. We have largely followed the procedures laid out by Pigulski et al. (2016), with a few deviations. First, ν Eri is not bright enough to require a correction for CCD nonlinearity. Second, whenever we noticed a temperature-dependent change of the correlations with x/y position we separated the data into smaller temporal subsets that were decorrelated individually. Third, in two cases an additional correction of the light curve was necessary due to variable background illumination due to scattered light, e.g. from the Moon. Finally, a few significant outliers were rejected. The rejected points had a probability of less than 50% to fall within the standard deviation of all data points. These outliers are suspected to be caused by blurred images or strong cosmic ray hits, and are very small in number ($< 0.2\%$ of all data points).

An overview of the characteristics of the data sets used for analysis is given in Table 2; the time base of the BRITE observations is somewhat above 170 d in both filters (including a ≈ 45 d gap in the blue-filter data). The precision of the measurements as given in this table was deduced from the rms scatter of the orbital means of the pulsation-filtered decorrelated light curves and must therefore be considered a lower limit to the real accuracy. Even though the measurements by the different satellites have varied quality, we decided against the application of statistical weights to the different data sets.

Due to the complexity of this reduction procedure, special care was taken to test its effects on the frequency analysis to follow. In other words, we checked whether the decorrelation could introduce spurious periodic signals. The first test consisted of introducing synthetic periodic signals into the BRITE light curves of ν Eri at frequencies deemed to be critical (the possible g-mode frequency domain between $0.1 - 0.9 \text{ d}^{-1}$, the Earth's rotation frequency 1 d^{-1} , and frequen-

Table 2. Log of the BRITE measurements of ν Eri. Start and end times of the individual satellites' observations are given as well as the number of one-minute data bins, the number of orbits observed, and the precision of the orbital means.

Satellite	T_{start}	T_{end}	# data		σ mmag
	HJD - 2456000		1-min	orb	
BAb	926.354	953.075	1453	198	4.6
BLb	998.527	1098.276	12536	1089	1.9
BTr	924.724	995.525	11753	676	1.1
BHr	972.718	1095.509	12802	1107	2.3

cies close to the known stellar oscillations). These modified light curves were decorrelated like the original ones. The result of this experiment was that the amplitudes of some of the artificial signals were suppressed (mostly within the errors), and that no additional spurious signals originated. The second test was to decorrelate the BRITE data of another star observed in the same field, γ Ori, deemed to be constant, the same way as the ν Eri light curves. The aim of this test was to check which frequency domains can be affected by imperfections in the data decorrelation process. Even though the exact correlations in the data may not necessarily be the same due to the variation of the PSF over the BRITE field of view (Pablo et al. 2016), the time scales at which reduction deficiencies will manifest themselves should be the same. We will compare the results for γ Ori and ν Eri in the next section.

Finally, part of the BAb measurements were of considerably poorer quality than the remainder of the BRITE photometry (above 8 mmag rms in the orbital means) due to temporal pointing instabilities. Hence these observations were not analysed further. For frequency analysis, all data were binned into one-minute and orbital means (if a sufficient number of observations was obtained during any given orbit). Some example light curves are shown in Fig. 1, that also demonstrates the different sampling of the space and ground-based data and the changes in the amplitude due to the beating of multiple pulsation periods.

3 FREQUENCY ANALYSIS

We analysed our data using the PERIOD04 software (Lenz & Breger 2005). This package applies single-frequency power spectrum analysis and simultaneous multi-frequency sine-wave least-square fitting. It also includes advanced options such as the calculation of optimal light-curve fits for multiperiodic signals including harmonic, combination, and equally spaced frequencies.

To assess the detection significance of any given signal, we adopted the widely used and reliable criterion by Breger et al. (1993, 1999). According to this criterion, any independent peak that exceeds a signal-to-noise (S/N) ratio of four in the amplitude spectrum is statistically significant, whereas any combination (sum or difference) frequency is considered detected when exceeding $S/N = 3.5$. To compute the noise level in the presence of frequency-dependent red noise, we integrated the amplitude spectrum in sliding windows over intervals of 2 d^{-1} .

However, before actually looking for pulsational signals

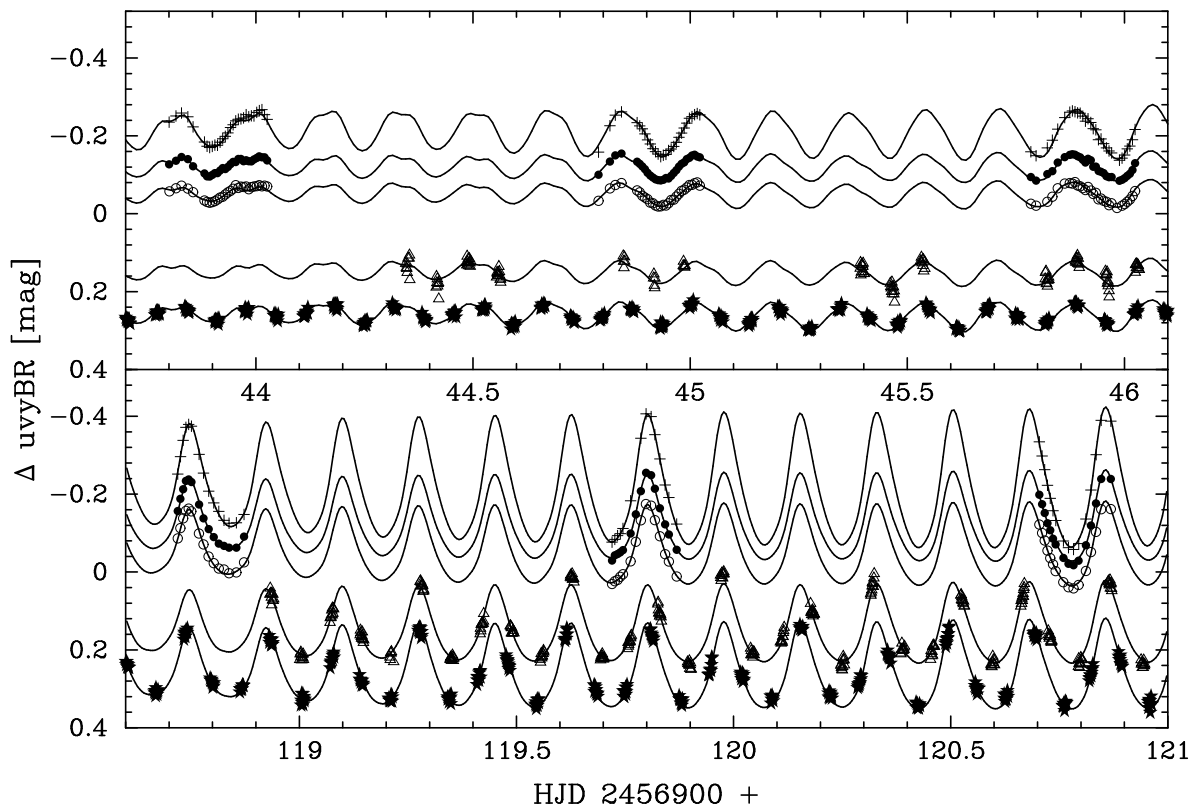


Figure 1. Some example light curves of ν Eri from our observations. The plus signs represent the u filter data, the full circles the v filter light curves, and the open circles the y filter light curves. The BRITE B observations are the open triangles (1-minute averages, upper panel: BAb, lower panel BLb), and the BRITE R observations marked with star symbols (1-minute averages, upper panel: BTr, lower panel BHR). The lines are multifrequency fits to the light curves to be computed in Sect. 3.

in the light curves, it is worthwhile to consider the characteristics of the data at hand. The BRITE observations are very close to being evenly spaced, causing strong aliasing at the orbital frequency. An example is shown in the upper panel of Fig. 2, which contains the spectral window function of the measurements by BHR. The alias peak at the orbital frequency has 96% of the amplitude of the zero-frequency input signal. Therefore analysing the data from a single satellite can easily result in mistakes in frequency detection.

This problem can be mitigated when data from more than one satellite are available. In the second panel of Fig. 2 the spectral window function of the combined data from the two red-filter BRITEs is shown. The alias at the orbital frequency is clearly diminished, as a consequence of the different orbits of the two satellites: their orbital periods are not exactly the same, and they do not observe at the same time. Figure 1 also illustrates this fact: in the lower panel it can be easily discerned that the observation window of BLb drifts with respect to that of BHR. Returning to Fourier space (Fig. 2, third panel), the orbital aliases can be suppressed even more when the data from all four BRITEs employed to observe ν Eri are combined.

As it is well known, a similar problem is present in ground-based observations due to the regular daytime gaps in the measurements. In the fourth panel of Fig. 2 we show the spectral window function of our ground-based observations; the well-known daily aliasing pattern is clearly present. It should be noted that adding the comparably small data set from SAAO to the APT data resulted in a

decrease of the $1d^{-1}$ alias from 91% to 76% of the central peak.

Because the aliasing structure of the space observations differs strongly from that of ground-based data, combining them results in an even stronger depression of the aliases (lowest panel of Fig. 2). Therefore, from the point of view of frequency detection it would be advantageous if such a combined data set could be exploited.

We thus examined how such a data set could be created, given that the amplitudes of the stellar variability are different from filter to filter, and that phase lags may occur between the light curves from different filters. Fortunately, for β Cep stars, both those amplitude differences and phase lags are not strong in the visual band. After some trials, we found that for ν Eri combining the BRITE measurements from all satellites with the ground-based y -filter data - for the purpose of frequency detection only - is the most useful approach. We note that for other stars or data/filter combinations the situation may be different and such an approach must always be made with great caution.

Consequently, we adopted the following frequency analysis strategy: we computed amplitude spectra of the combined data (using orbital means of the BRITE measurements) and identified the significant signals step by step. These were fitted to the data, using the 1-minute binned BRITE data to not falsify the amplitudes of the higher-frequency signals. We adopted the same frequencies for all filters, but determined the amplitudes and phases from the data sets in the individual filters separately before comput-

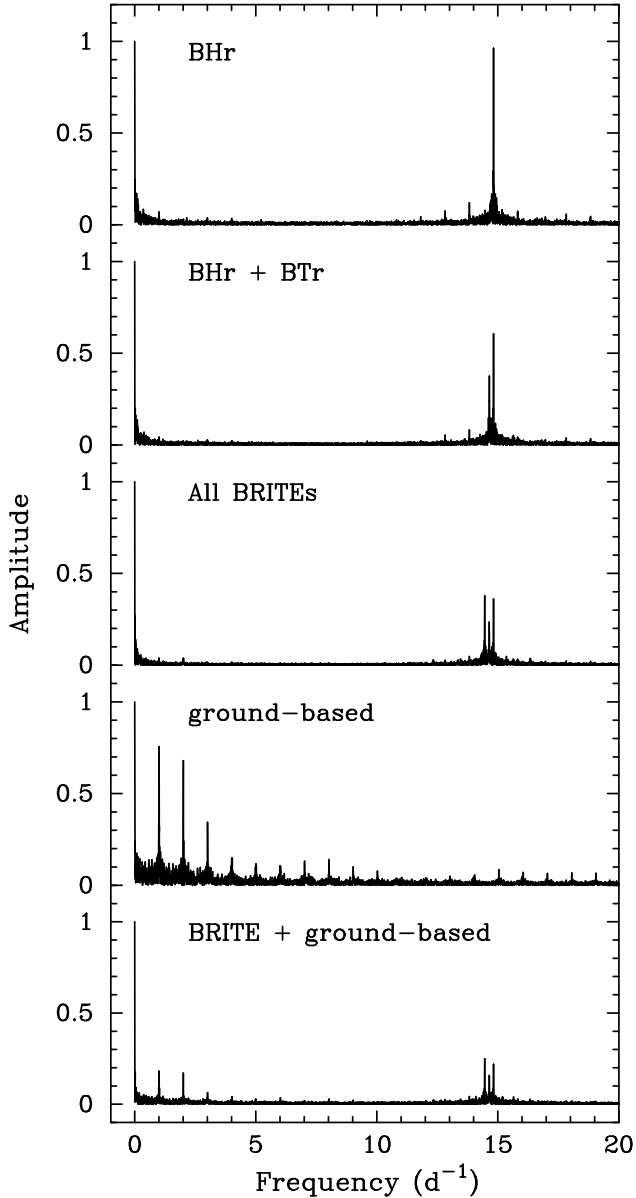


Figure 2. Uppermost panel: spectral window function of the BHR data only. Second panel: the same, but for the combined red-filter BRITE data. Third panel: the same, with all red- and blue-filter BRITE data combined. Fourth panel: spectral window for the ground-based y -filter measurements. Fifth panel: spectral window for the merged BRITE and ground-based data.

ing orbital averages and combining the residuals again. Then we searched for more stellar variability frequencies; we call this procedure prewhitening. The parameters of the newly detected periodic signals were optimized together with those found previously. Once no significant variation was left in the residuals, the analysis was terminated.

Figure 3 illustrates this process. In the uppermost panel a spectral window is shown as the Fourier transform of a single noise-free sinusoid with a frequency of 5.7633 d^{-1} (the strongest pulsational signal of ν Eri) and an amplitude of 36 mmag sampled in the same way as were our measurements. As expected, aliasing is strongly suppressed.

The amplitude spectra of the data itself (second panel

of Fig. 3) shows the signal designated f_1 as the strongest, but some additional structures not compatible with spectral window sidelobes are also present. Consequently, we prewhitened this signal as described before, and computed the amplitude spectrum of the residual light curve (third panel of Fig. 3).

This resulted in the detection of a second signal (f_2) and of another variation at the sum frequency of the two previously detected. We then prewhitened a three-frequency fit from the data using the same optimisation method as before and fixed the combination term to the exact sum of the two independent frequencies within PERIOD04. The next panels show the continuation of this process until the detection of 32 frequencies, all of which are significant within the criteria discussed before.

The lowest panel of Fig. 3 shows the amplitude spectrum of the BRITE data for γ Ori, a constant star as far as we can tell. Comparing it with the amplitude spectrum of ν Eri prewhitened by 32 frequencies, it can be concluded that possible artifacts left behind in the reduction procedure only seem to occur in confined frequency ranges: below 0.2 d^{-1} , between $0.95 - 1.1 \text{ d}^{-1}$, and around the orbital aliases of these frequency domains (or vice versa). The frequencies detected for ν Eri are outside these domains, with the exception of the two lowest-frequency combinations. However, as these are also present in the ground-based data, there is no reason to doubt their reality.

The final results of the frequency analysis of our ν Eri data, with the amplitudes determined for the individual filters separately, are listed in Table 3. This listing contains 40 signals, which is more than the 32 frequencies prewhitened in Fig. 3. The additional eight signals are low-amplitude combination frequencies only. The designation of the independent frequencies was chosen to be consistent with JHS and Handler et al. (2004).

The residuals from this solution were searched for other signals that may be intrinsic to the star. We analysed the amplitude-scaled residuals in the different filters (whereby the u data were divided by 1.5, the v and B data divided by 1.05, and the R data multiplied by 1.05 to scale them to amplitudes similar to that in the y filter), and using different combinations of data sets. Even though some interesting possibilities for further intrinsic pulsation frequencies offered themselves, we prefer to err on the side of caution and stop the frequency search at this point.

Nevertheless, it is interesting to note that the residual scatter in the light curves (6.4 mmag per point in u , 5.2 mmag /point in v , 4.5 mmag /point in y , 5.5 mmag /orbit in B , and 4.2 mmag /orbit in R) is larger than the precision of the observations. This may be partly explicable by data reduction imperfections, but residual intrinsic stellar variability is likely also involved.

4 MODE IDENTIFICATION

BRITE-Constellation was designed to obtain multicolour time-series photometry specifically to provide identifications of the spherical degree l of the modes of pulsating stars (Weiss et al. 2014). Daszyńska-Daszkiewicz (2008) provided diagnostic diagrams to perform such mode identifications

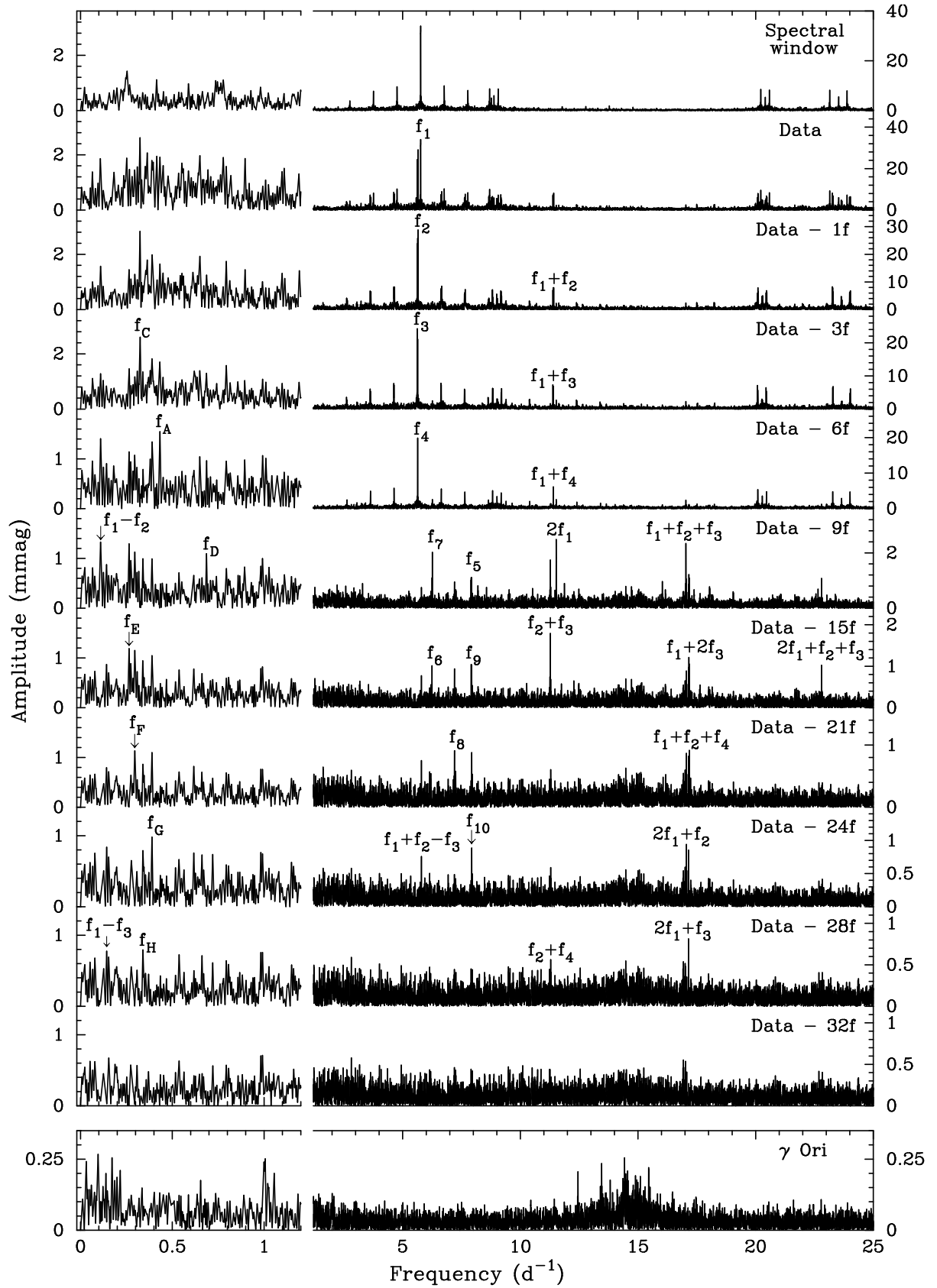


Figure 3. Amplitude spectra of ν Eri. The uppermost panel shows the spectral window of the data, followed by the periodogram of the data. Successive prewhitening steps are shown in the following panels; note their different ordinate scales. Also note that the low-frequency domain is shown in higher resolution, and that the lowest panel shows the amplitude spectrum of the supposedly constant star γ Ori for comparison. The latter is not as “flat” as it is dominated by reduction imperfections rather than by white noise.

Table 3. Multifrequency solution for our time-resolved photometry of ν Eri. Formal error estimates (following Montgomery & O’Donoghue 1999) for the independent frequencies are also quoted. Formal errors on the amplitudes are ± 0.3 mmag in u and ± 0.2 mmag in v , y , B , and R . These formal errors are known to underestimate the real errors by about a factor of two (Handler et al. 2000, JHS). The S/N ratio quoted is for the data set used to create Fig. 3. The detected signals are separated in groups of independent pressure and mixed modes (numerical subscripts), gravity modes (letter subscripts), as well as first, second and third-order combination frequencies, respectively.

ID	Freq. (d^{-1})	u Ampl. (mmag)	v Ampl. (mmag)	y Ampl. (mmag)	B Ampl. (mmag)	R Ampl. (mmag)	S/N
f_1	5.763264 ± 0.000012	68.0	38.3	34.4	37.6	33.0	262.8
f_2	5.653917 ± 0.000015	39.6	27.5	26.2	27.7	25.8	195.9
f_3	5.620047 ± 0.000017	34.8	24.4	23.1	24.7	22.8	173.5
f_4	5.637247 ± 0.000019	31.3	22.3	20.9	22.3	20.6	156.8
f_5	7.8995 ± 0.0004	1.4	1.1	1.1	0.9	0.9	7.0
f_6	6.2434 ± 0.0003	1.4	1.0	0.9	1.2	1.3	8.4
f_7	6.2618 ± 0.0002	2.8	2.0	1.8	2.4	1.9	15.2
f_8	7.2026 ± 0.0004	1.4	1.3	1.2	1.0	0.7	7.3
f_9	7.9131 ± 0.0004	1.3	1.0	0.8	1.3	0.9	6.9
f_{10}	7.9307 ± 0.0004	1.3	1.3	1.2	0.8	1.0	7.0
f_A	0.4307 ± 0.0003	3.0	1.5	1.6	1.3	1.2	5.7
f_C	0.3242 ± 0.0002	3.8	2.4	2.1	3.3	3.2	11.7
f_D	0.6870 ± 0.0004	2.2	1.3	1.5	0.8	1.1	4.4
f_E	0.2648 ± 0.0004	2.4	1.3	1.5	1.6	1.0	5.2
f_F	0.2951 ± 0.0004	3.2	1.7	1.7	0.8	1.1	4.5
f_G	0.3894 ± 0.0004	2.4	1.6	1.6	0.9	0.7	4.3
f_H	0.3395 ± 0.0005	2.4	1.3	1.3	0.7	1.0	4.0
$f_1 - f_2$	0.1093473	3.4	2.0	2.4	0.6	1.0	5.0
$f_1 - f_3$	0.1432171	2.1	1.1	1.3	0.6	0.5	3.6
$f_3 + f_4$	11.257294	0.7	0.8	0.5	0.6	0.3	3.6
$f_2 + f_3$	11.273963	2.3	1.5	1.7	1.9	1.6	13.0
$f_2 + f_4$	11.291164	0.6	0.6	0.5	0.5	0.5	3.5
$f_1 + f_3$	11.383311	9.3	6.9	6.6	7.1	6.5	49.2
$f_1 + f_4$	11.400511	9.7	7.1	6.6	6.8	6.3	47.1
$f_1 + f_2$	11.417181	12.1	9.1	8.5	8.6	8.2	58.7
$2f_1$	11.526528	4.3	2.9	2.6	2.9	2.6	18.5
$f_1 + f_2 - f_3$	5.7971337	0.8	0.9	0.7	1.0	0.7	5.6
$f_2 + f_3 + f_4$	16.911211	0.7	0.4	0.6	0.5	0.4	3.5
$2f_2 + f_3$	16.927880	1.4	1.1	1.0	0.5	0.4	4.4
$f_1 + 2f_3$	17.003358	0.8	0.6	0.5	0.5	0.4	3.5
$f_1 + f_3 + f_4$	17.020558	1.0	0.6	0.7	1.1	0.5	4.9
$f_1 + f_2 + f_3$	17.037227	3.7	2.6	2.2	2.3	2.1	19.5
$f_1 + f_2 + f_4$	17.054428	1.0	0.9	1.0	1.3	0.7	8.3
$f_1 + 2f_2$	17.071097	0.8	0.6	0.7	0.2	0.6	3.9
$2f_1 + f_3$	17.146575	1.2	0.8	0.9	1.1	0.8	7.4
$2f_1 + f_4$	17.163775	1.5	1.3	0.9	0.9	0.9	9.1
$2f_1 + f_2$	17.180444	1.3	1.2	0.8	1.5	1.1	8.5
$f_1 + 2f_2 + f_3$	22.691144	0.4	0.4	0.3	0.6	0.5	3.9
$2f_1 + f_2 + f_3$	22.801022	1.6	0.9	1.1	1.1	1.1	10.3
$2f_1 + 2f_2$	22.834361	0.3	0.2	0.2	0.6	0.2	4.0

from a comparison of the amplitude ratios and phase shifts between the two BRITE passbands.

The four strongest modes of ν Eri are both spectroscopically and photometrically uniquely identified (Handler et al. 2004, De Ridder et al. 2004, Daszyńska-Daszkiewicz & Walczak 2010): the strongest mode is radial (spherical degree $l = 0$) and the high-amplitude triplet consists of dipole modes ($l = 1$). In Fig. 4, the observed $uvyBR$ amplitude ratios are compared to theoretical predictions for the used Strömgren and BRITE passbands for these four modes.

The theoretical amplitude ratios were computed with

the method of Balona & Evers (1999), using the nonadiabatic f parameter (which is the ratio of the amplitude of the bolometric flux variations to the radial displacement at the photosphere level) calculated from theoretical models, and an arbitrary user supplied value of the pulsational radial velocity variation to be translated to photometric amplitudes. Pulsation modes with nonadiabatic frequencies between $5.3 - 6.0 \text{ d}^{-1}$ were considered because the amplitude ratios are sensitive to the radial overtone of the modes. This approach is in principle the same as that of Daszyńska-Daszkiewicz (2008), and we have verified that the outcome

of our calculations (based on older model atmospheres) is consistent with hers. The parameters used for ν Eri are consistent with the seismic models by Pamyatnykh et al. (2004), i.e. the f parameters were taken from stellar models of 9.5 and 10 M_{\odot} in a temperature range of 22000 ± 600 K. The results from non-LTE model atmosphere analysis of ν Eri by Nieva & Przybilla (2012, $T_{\text{eff}} = 22000 \pm 400$ K, $\log g = 3.85 \pm 0.05$) are in excellent agreement with this choice. The ranges in the adopted parameters translate into the error bars of the theoretical amplitude ratios indicated in Fig. 4.

There are no big surprises in the mode identification: the literature results are confirmed. However, a closer look at the visual amplitude ratios alone (i.e. excluding the u filter) reveals that for both $l = 0$ and $l = 1$ models predict a steeper increase in amplitude towards shorter wavelengths than observed. This is better seen in a comparison of observed and theoretical amplitude ratios and phase shifts for the optical v/y and B/R filter combinations (Fig. 5) computed with the same parameters as specified above; we shall discuss this result in Sect. 5.

Because of their low amplitudes, identifying the l value of the remaining modes from our data does not result in an improvement over results in the literature. We refer to the study by Daszyńska-Daszkiewicz & Walczak (2010) for observational identifications of these modes.

5 DISCUSSION

Compared to previous results, in particular to the work by JHS, there are several differences. These authors reported 36 frequencies in their light curves, of which two originated from the main comparison star. The present study revealed 40 frequencies of light variation, all of them due to ν Eri.

Among the independent frequencies that would correspond to β Cep-type p modes, the present work has ten in common with JHS. We do not detect their two weakest signals in this domain, at 6.2236 and 6.7332 d^{-1} . The first signal has been found in other studies, particularly in the spectroscopic analysis by Aerts et al. (2004), which raises the suspicion that its amplitude has dropped below the present detection level. Searching for a signal at this frequency yielded a null result. Concerning the 6.7332 d^{-1} signal, we cannot find a trace of it.

As just mentioned, some of the stellar pulsational signals change their amplitudes, apparently even to the extent that they can sometimes be detected, but sometimes disappear beyond the observational detection threshold. The differences between the independent pulsation frequencies and amplitudes as derived by JHS and us, and common to both studies, are summarized in Table 4.

It becomes clear that the amplitude of the strongest mode has considerably dropped compared to the results by JHS - by some 6% over the last decade. Therefore these amplitude variations are not a simple consequence of the interference of low-amplitude pulsation modes with observational noise, but are intrinsic to the star. On the other hand, the amplitudes of the $f_2 - f_4$ triplet appeared fairly constant, aside from a slight increase of the amplitude of mode f_2 compared to the study by JHS.

We recall that Handler et al. (2004) already argued in

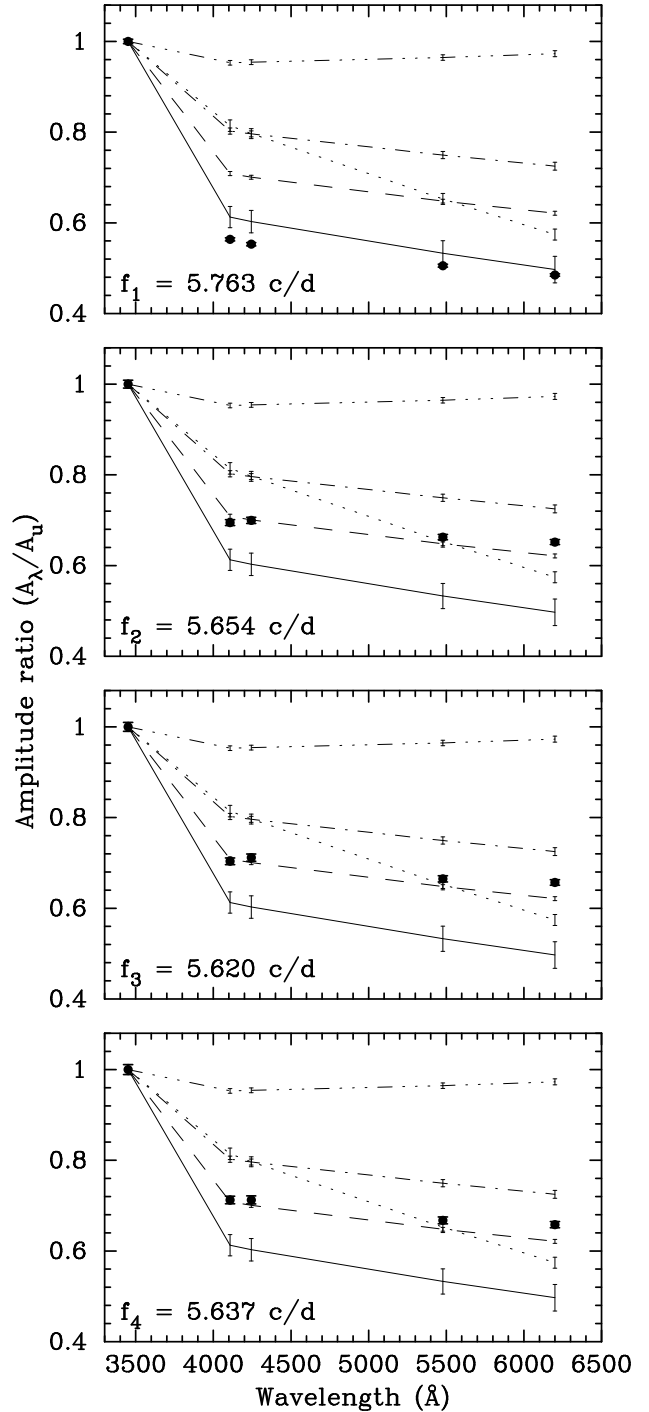


Figure 4. Identification of the spherical degree of the four strongest pulsation modes of ν Eri. The filled circles with error bars are the observed amplitude ratios, in order of increasing wavelength u/u , v/u , B/u , y/u and R/u . The full lines are theoretical predictions for radial modes, the dashed lines for dipole modes, the dashed-dotted lines for quadrupole modes, the dotted lines for $l = 3$ modes, and the dashed-dot-dot-dotted lines are for $l = 4$. The thin error bars delineate the uncertainties in the theoretical amplitude ratios.

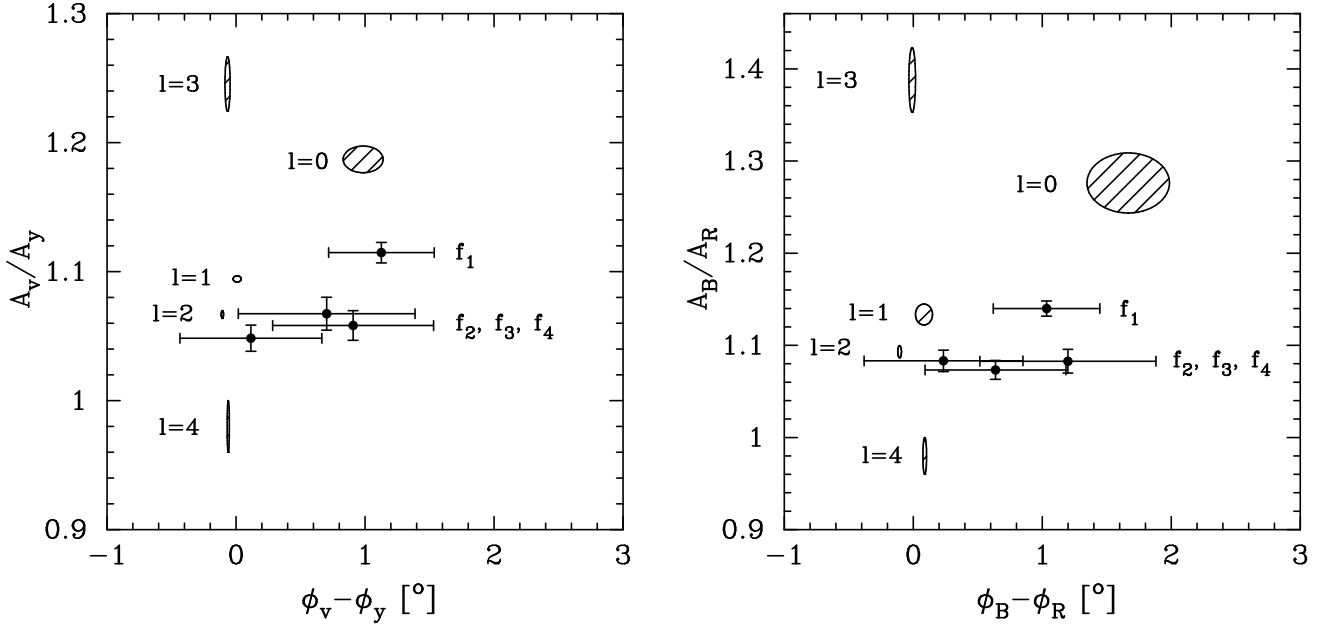


Figure 5. Identification of the spherical degree of the four strongest pulsation modes of ν Eri from optical filters only. The shaded areas delineate the theoretically predicted domains of modes depending on their spherical degree (note that some of these are very small), whereas the filled circle with the error bars are the observed loci of the radial mode f_1 and the dipole modes $f_2 - f_4$.

Table 4. Changes in the pulsational amplitudes and frequencies of ν Eri between the study of JHS and the present one. The values were calculated as JHS *minus* present.

ID	Δf (10^{-3}d^{-1})	Δu (mmag)	Δv (mmag)	Δy (mmag)
f_1	-0.019 ± 0.012	-4.8 ± 0.3	-2.5 ± 0.2	-2.3 ± 0.2
f_2	$+0.040 \pm 0.015$	$+1.1 \pm 0.3$	$+0.4 \pm 0.2$	$+0.8 \pm 0.2$
f_3	$+0.028 \pm 0.017$	-0.2 ± 0.3	-0.1 ± 0.2	-0.1 ± 0.2
f_4	$+0.000 \pm 0.019$	-0.5 ± 0.3	$+0.0 \pm 0.2$	-0.1 ± 0.2
f_5	$+1.3 \pm 0.4$	-2.2 ± 0.3	-1.5 ± 0.2	-1.4 ± 0.2
f_6	-0.4 ± 0.3	-1.6 ± 0.3	-0.9 ± 0.2	-1.2 ± 0.2
f_7	-1.1 ± 0.2	$+0.0 \pm 0.3$	$+0.0 \pm 0.2$	$+0.0 \pm 0.2$
f_8	$+1.7 \pm 0.4$	$+0.0 \pm 0.3$	$+0.4 \pm 0.2$	$+0.3 \pm 0.2$
f_9	-0.7 ± 0.4	-0.4 ± 0.3	-0.1 ± 0.2	-0.4 ± 0.2
f_{10}	$+0.8 \pm 0.4$	$+0.1 \pm 0.3$	$+0.4 \pm 0.2$	$+0.3 \pm 0.2$
f_A	-2.1 ± 0.3	-1.1 ± 0.3	-1.0 ± 0.2	-0.9 ± 0.2

favour of some amplitude variation occurring in the pulsation spectrum of ν Eri. In this context it is interesting to note that an amplitude *increase* of f_1 with respect to the measurements by van Hoof (1961), analysed by Cuypers & Goossens (1981), had occurred, and that the relative amplitudes within the $f_2 - f_4$ triplet had also changed.

As regards to the remaining modes, decreases in the amplitudes of modes f_5 , f_6 and f_A are also present at a significant level. The amplitudes of modes f_7 through f_{10} stayed the same within the errors, keeping in mind that our error bars likely underestimate the real uncertainties.

Turning to the independent low frequencies (ν Eri is a hybrid p and g-mode pulsator), considerable changes have occurred since the work of JHS. A previously unknown signal f_C now dominates the low-frequency domain. On the other hand, the low-frequency signal f_B by JHS is no longer detectable at all, and the amplitude of signal f_A has dropped to about 2/3 of its previous value. The frequency of this signal has also considerably shifted. The biggest change com-

pared to the results of JHS, however, is the detection of a total of six new low-frequency independent modes ($f_C - f_H$). Had these signals been present with similar amplitudes in the old data, most of them would have been detected, as a re-examination of this data set shows. One may suspect that the decrease in amplitude of several of the p modes, in the sense that the pulsational energy lost by the p modes became available to raise the amplitudes of these g modes.

The newly detected g modes make it tempting to look for equal frequency splittings indicative of the rotation rate in the stellar interior, particular when recalling the result by Pamyatnykh et al. (2004) that ν Eri rotates some four times more rapidly near the core than on its surface. However, the theoretically predicted g-mode frequency spectrum (e.g., see Fig. 6 of Daszyńska-Daszkiewicz & Walczak 2010) of ν Eri is very dense. Even in the small frequency region between $0.26 - 0.43 \text{d}^{-1}$ in which we detected six g modes, models predict 13 radial overtones of $l = 1$ g modes. Any claim of rotational splitting in the g-mode domain must therefore remain in the realm of speculation. On the other hand, it can at the same time also be speculated that the apparent change in frequency of mode f_A may actually be a manifestation of a different mode present in the current data set.

Moving on to the combination frequencies, our results are mostly consistent with those by JHS (apart from some amplitude variations) as far as the first-order combinations are concerned, apart from us not detecting $2f_2$, $f_1 + f_5$ and $f_1 - f_4$, but $f_1 - f_3$ instead. We detect all the higher-order combination frequencies as did JHS, and add five more due to our lower detection limit.

Two δ Scuti-type oscillation frequencies (10.874 and 17.252d^{-1}) originating from the comparison star ξ Eri were reported by JHS; the lower-frequency of them was preliminarily mentioned by Handler et al. (2004). The latter signal can be discerned in our present ground-based photometry

using the same comparison star, but does not occur at a significant level. We were unable to find the higher-frequency variation reported by JHS. We caution that our new ground-based data are considerably fewer than those reported by JHS, which may explain these differences.

We reported that the theoretically predicted pulsation amplitude-wavelength relation in the visual range is steeper than that observed (Fig. 4). This raises the suspicion that the filter bandpasses we used for the calculations may be inaccurate. That the effect is systematic over the visual wavelength range covered by our measurements (4100 – 6200 Å), i.e. not only one or two filters in the optical are affected, argues against such an interpretation, however. The same argument refutes that the problem stems from imperfections in the data reduction procedure; furthermore the ground-based and space photometry were reduced independently.

Figure 5 shows the discrepancy more drastically. The comparison of the theoretical loci of low- l pulsation modes and the observed ones using combinations of two optical filters only and the observed positions of the well-identified modes $f_1 - f_4$ shows some large discrepancies as far as the amplitude ratios are concerned. Using these diagrams, the radial mode f_1 would rather be identified as a dipole, whereas the $l = 1$ modes $f_2 - f_4$ are located where $l = 2$ modes would be expected. Since this problem does arguably not originate from poorly known filter bandpasses, another explanation in physical terms needs to be sought.

For instance, rapid stellar rotation would change the temperature and mode amplitude distribution on the stellar surface. Hence amplitude ratios between different filters would become dependent on the inclination of the rotation axis to the line of sight, the rotation rate, and the azimuthal order of the modes and can deviate considerably from the non-rotating case (e.g., Reese et al. 2013). However, ν Eri is an intrinsically slow rotator (Pamyatnykh et al. 2004) with a surface rotation period of about two months, and such a possibility can hence be ruled out.

The pulsation amplitudes of ν Eri are relatively high and therefore harmonic and combination frequencies are observed. One may therefore surmise that nonlinear effects could modify the amplitudes, which would be unaccounted for by the models used to compute the theoretical amplitude ratios. Indeed, the dominant modes of another β Cep star with prominent harmonics and combination frequencies, 12 Lac (Handler et al. 2006) also have smaller amplitude ratios in the optical than theoretically predicted. On the other hand, stars with weak or no harmonics and combination frequencies with well-identified oscillations (e.g. IL Vel and KZ Mus, Handler et al. 2003., V2052 Oph, Handler et al. 2012) do not seem to show this effect, whereas it may be suspected in others (V836 Cen, Dupret et al. 2004).

Another possibility is that there is a problem with the theoretical predictions of the pulsation amplitude vs. wavelength relation. We may for instance just have used non-optimal stellar input parameters. However, in such a situation it would be hard to understand why the amplitude ratios with respect to the Strömgren u filter were quite well reproduced. For instance, an incorrectly adopted effective temperature would cause a systematic change of the predicted amplitude ratios within all passbands as they are all located in the Rayleigh-Jeans tail of the stellar spectral energy distribution. We recall that the effective temperature

adopted for our calculations is in perfect agreement with recent and modern spectral analyses (Nieva & Przybilla 2012).

One more possible culprit would be a poor choice of the complex f parameter that is a vital ingredient for the computation of theoretical pulsation amplitude ratios. As pointed out by, e.g., Daszyńska-Daszkiewicz & Walczak (2010), this parameter is very sensitive to the metal content and opacities in the stellar atmosphere. We have therefore made some experiments with modifying the f parameter, e.g. by adopting empirically determined values (Daszyńska-Daszkiewicz & Walczak 2010) instead of the ones predicted by stellar models. Our experiments did not bear fruit, but more trials in this direction are advised. In any case, any seismic model that contains or proposes modifications to the f parameter should also reproduce the observed amplitude ratios.

To conclude, we cannot offer a good explanation for the discrepancy between the observed and theoretical pulsational amplitude ratios for the dominant modes of ν Eri in the optical at this point. However, we do want to stress that identifying pulsational modes of β Cep stars from optical amplitude ratios (and phase shifts) alone may be misleading, at least until this problem has been resolved.

6 SUMMARY AND CONCLUSIONS

We have reported the first combined analysis of simultaneous BRITe-Constellation and ground-based photometry. The measurements were acquired for the well-studied β Cep star ν Eri, with a combined duration of 173.5 d. This exemplary data set was used to show the power of joining these two types of observations, because they complement each other well in terms of suppressing aliasing problems in the data; aliasing is practically non-existent if the data can be carefully analysed together.

Performing such a frequency analysis, we detected 40 signals in the light curves. Among these are six newly discovered gravity-mode frequencies. Their detection is a consequence of the combination of, firstly, the lower noise level in the BRITe data, which amounts to 72% between 0 – 1 d⁻¹ and 80% between 5 – 9 d⁻¹ of that in the combined 2002 – 2004 ground-based multisite photometry (JHS). The second factor is the evolution of the stellar pulsation amplitudes. Such changes in the stellar mode spectrum make frequency analyses more challenging, but are also an asset as repeated observations may reveal more seismic information. Unfortunately, the data set reported here cannot be analysed together with those from the multisite campaigns carried out more than a decade ago (JHS) as the temporal gap between the two observational campaigns is too large, and just because the amplitude variations have occurred. However, at least some of the BRITe satellites will continue to observe ν Eri, and eventually this gap can be bridged.

We showed that the observed pulsational amplitude ratios for the strongest modes are consistent with their previous identifications. However, the amplitude-wavelength relation in visual passbands is flatter than that predicted from theory. Although we cannot offer a good explanation for this discrepancy at this point, we suggest that mode identification of β Cep stars should not be done in the optical alone; a UV band or radial velocities are necessary.

The pulsation amplitude-wavelength relation observed for ν Eri requires theoretical explanation to derive reliable mode identifications from BRITE data alone. Furthermore, the additional gravity modes detected in the present work call for explanation, as current pulsation models have difficulties to excite them. An upcoming theoretical study by Daszyńska-Daszkiewicz et al. (2016) will address these questions.

ACKNOWLEDGEMENTS

This work has been supported by the Polish NCN grants 2011/01/B/ST9/05448, 2011/01/M/ST9/05914, 2011/03/B/ST9/02667 and 2015/18/A/ST9/00578. TR acknowledges support from the Canadian Space Agency grant FAST. GAW and SMR acknowledge Discovery Grant support from the Natural Science and Engineering Research Council (NSERC) of Canada. AFJM is grateful for financial aid from NSERC and FQRNT (Quebec). KZ acknowledges support by the Austrian Fonds zur Förderung der wissenschaftlichen Forschung (FWF, project V431-NBL). BTr operations are supported through a Canadian Space Agency (CSA) Academic Development grant.

This paper has been typeset from a $\text{\TeX}/\text{\LaTeX}$ file prepared by the author.

REFERENCES

- Aerts C., et al., 2004, MNRAS 347, 463
 Ausseleloos M., Scuflaire R., Thoul A., Aerts C., 2004, MNRAS 355, 352
 Balona L. A., Evers E. A., 1999, MNRAS 302, 349
 Breger M., et al., 1993, A&A 271, 482
 Breger M., et al., 1999, A&A 349, 225
 Buysschaert B., et al., 2016, A&A, in preparation
 Cuyper J., Goossens M., 1981, A&AS 45, 487
 Daszyńska-Daszkiewicz J., 2008, Comm. Asteroseism. 152, 140
 Daszyńska-Daszkiewicz J., Walczak P., 2010, MNRAS 403, 496
 Daszyńska-Daszkiewicz J., Pamyatnykh A. A., Walczak P., Colgan J., Fontes C., Kilcrease D., 2016, MNRAS, in preparation
 De Ridder J., et al., 2004, MNRAS 351, 324
 Dupret M.-A., Thoul A., Scuflaire R., Daszyńska-Daszkiewicz J., Aerts C., Bourge P.-O., Waelkens C., Noels A. et al., 2004, A&A 415, 251
 Dziembowski W. A., Pamyatnykh A. A., 2008, MNRAS 385, 2061
 Handler G., et al., 2000, MNRAS 318, 511
 Handler G., Shobbrook R. R., Vuthela F. F., Balona L. A., Rodler F., Tshenye T., 2003, MNRAS 341, 1005
 Handler G., et al., 2004, MNRAS 347, 454
 Handler G., et al., 2006, MNRAS 365, 327
 Handler G., et al., 2012, MNRAS 424, 2380
 van Hoof A., 1961, Z. Astrophys., 53, 106
 Jerzykiewicz M. et al. 2005, MNRAS 360, 619 (JHS)
 Jerzykiewicz M. et al. 2013, MNRAS 432, 1032
 Lenz P., Breger M., 2005, Comm. Asteroseism. 146, 53
 Montgomery, M. H., O'Donoghue, D., 1999, Delta Scuti Star Newsletter 13, 28 (University of Vienna)
 Nieva M.-F., Przybilla N., 2012, A&A 539, A143
 Pablo H., et al. 2016, PASP, in press (arXiv:1608.00282)
 Pamyatnykh A. A., Handler G., Dziembowski W. A., 2004, MNRAS 350, 1022
 Pigulski A. et al. 2016, A&A 588, 55

- Popowicz A. 2016, Proc. SPIE 99041R (doi:10.1117/12.2229141)
 Popowicz A. et al. 2016, in preparation
 Reese D. R., Prat V., Barban C., van 't Veer-Menneret C., MacGregor K. B., 2013, A&A 550, 77
 Stankov A., Handler G., 2005, ApJS 158, 193
 Weiss W. W. et al., 2014, PASP 126, 573